SIMULACIJA VRTLOGOM UZBUĐENIH VIBRACIJA ŽIČARE SA DVA ČELIČNA UŽETA
SIMULATION OF VORTEX EXCITED VIBRATIONS OF A BICABLE ROPEWAY

Klaus HOFFMANN - Radostina PETROVA

Sažetak: *U radu se razmatra jedna od brojnih pojava odziva iz područja interakcije fluida i strukture, tj. vrtlogom uzbuđene vibracije. Napravljen je dinamički model istraživane žičare sa dva čelična užeta. Matematičke jednadžbe su izvedene i riješene pomoću numeričke simulacije. Predložena je metodologija za istraživanje zračnim vrtlogom uzbuđenih vibracija žičare. Svi rezultati, dobiveni tijekom simulacija, su uspoređeni sa eksperimentalnim rezultatima pri čemu podudarnost zadovoljava inženjerske kriterije. Predloženi modeli su intuitivni za korisnike i fleksibilni te je stoga potaknuta njihova primjena za znanstvene i inženjerske potrebe.*

Ključne riječi: − žičara sa dva čelična užeta
                      − uzbuda vrtlogom
                      − numerička simulacija

Abstract: *The presented work discusses one of the many response phenomena in the field of fluid–structure interaction, i.e. vortex-excited vibrations. The dynamic model of the examined bicable ropeway is created. Mathematical equations are derived and solved by means of numerical simulation. A methodology for studying the vortex-excited vibrations in aerial ropeways is suggested. All results, obtained during the simulation, are compared to experimental data and the coincidence satisfies the engineering criteria. The proposed models are user-friendly and flexible and thus their applicability for scientific and engineering purposes is actuated.*

Keywords: − bicable ropeway
               − vortex excitation
               − numerical simulation

1. INTRODUCTION

The interaction between a fluid flow and an embedded elastic body is extremely complex. Different response modes and flow phenomena exist depending on the flow characteristics, the body geometry and the structural properties like stiffness and damping. An essential requirement in the design of modern engineering structures, including ropeways, is to assess the influence of wind forces on structural response. This highlights the importance of understanding the phenomena, which determine the interaction between wind and structure and the need for reliable methods of its analysis. Today several different response phenomena in the field of fluid-structure interaction have been identified and grouped into response and stability problems. During the 18th and 19th century, various discoveries led to a better understanding of the factors that have an influence on the movement of solid bodies through air. By the early 1800s the relationship between resistance and the viscous properties of a fluid had been discovered, but it was not until the experiments of Reynolds in the 1880s that the significance of viscous effects was fully appreciated. Parallel to this, Strouhal [1] had already investigated the vortex shedding process on a circular cylinder and formulated a dimensionless shedding frequency now widely known as the Strouhal number. In 1911, von Kármán made an analysis of the alternating double row of vortices behind a bluff body fluid stream, now famous as von Kármán Vortex Street, [2].

The vibration phenomena found in bluff body aerodynamics are numerous and it is fruitful to group them by their origin and major characteristics. One such classification was proposed by Naudascher and Rockwell who distinguish 3 types of flow induced excitation as:

 • Extraneously induced excitation (e.g. periodic pulsation of oncoming flow);

 • Instability-induced excitation (flow instability inherent to the flow created by the structure under consideration), e.g. excitation induced by the von Kármán street;

 • Movement-induced excitation (fluid forces arising from the movement of the body or eventually of a fluid oscillator), e.g. galloping.

It should be noted that these forces can act simultaneously.

When a bluff body is embedded in a fluid flow, it may cause a wake to form behind the body. In the wake, the flow is turbulent but a distinguished pattern of vortices can usually be seen. These vortices are shed from the surfaces of the body and are then carried downstream. It is this shedding of vortices that induces an unsteady force on the body perpendicular to the undisturbed flow direction. The nature of the vortex shedding, particularly the frequency thereof, is determined largely by the geometry of the body, the speed of flow and the density and viscosity of the fluid. If the body is not rigidly mounted but has a degree of freedom associated with certain stiffness in the direction of the periodic force it will exercise an oscillation due to its inertia and the forcing action. If the natural frequency is close to the shedding frequency, resonance will occur. These vortex-induced vibrations can also be experienced by ropeways as will be discussed later on. They may, generally, be overcome by either changing the geometry of the structure (the gondola or the entire span) to shift the natural frequency away.

2. THE VORTEX SHEDDING PROCESS

The process of vortex shedding, ([3] and [4]) can only be explained if the effect of viscosity is considered. Only a viscous fluid will satisfy a no-slip condition of its particles on the surface of a body immersed in the flow [5]. Even if the viscosity is very small, this condition will hold but its influence on the flow regime will be confined to a small region: the boundary layer along the body. Within this boundary layer the velocity of the fluid changes from zero on the surface to the free-stream velocity of the flow. Whilst the free stream is pulling the boundary layer forward the skin friction at the solid wall is retarding it. At surfaces with high curvature, there can also be an adverse pressure gradient adding to the retarding action, which may cause the flow to be interrupted entirely and the boundary layer may detach from the wall. This is called separation.

In slender structures, regular vortex shedding may occur if the separation line is nearly straight. This is always the case in structures with straight corners or in a circular cylinder at special Reynolds numbers. The principle of the vortex shedding is shown in Figureure 1.

The flow separation on the right side (in the flow direction) produces a circulation, $+\Gamma$, in the wake of the cylinder. According to Thomson's vortex law, a counter circulation, $-\Gamma$, occurs around the cylinder, which produces a circulation flow Δu, clockwise around the cylinder. This velocity Δu, reduces the spatial velocity u_2 on the right side and increases u_2 on the left side. According to the Bernoulli equation, the static pressure

increases on the right side and decreases on the left side, so that a cross wind force, W_K, occurs, acting to the cylinder.

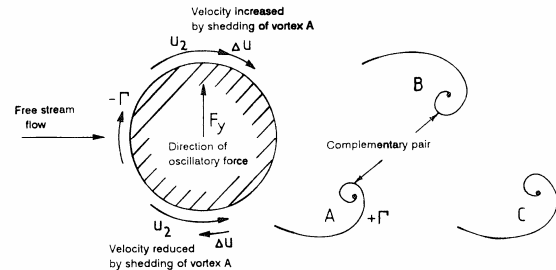With alternative vortex shedding this force, W_K,

Figure 1. The Principle of the Vortex Shedding at a Circular Cylinder [4]

alternates, too. If the cylinder is flexible in the cross flow direction and if its natural frequency is near the vortex shedding frequency, the exciting force, W_K, comes into resonance with cylinder vibration and this effect is called "vortex resonance". A typical phenomenon of vortex resonance is the "locking-in effect". The vortex shedding becomes synchronized with the vibration frequency at amplitudes of more than 2 or 3 % of the diameter, that means that the vortex shedding frequency ceases to follow the Strouhal law but is instead constant over a specific range of wind speed (Figure 2). The bandwidth of the resonance response of the structure is broadened; consequently the vibration becomes more stable and is less disturbed by wind velocity fluctuations. However, it is important to note, that even in the case of resonance, the amplitude always remains limited (Figure 2), which was for example shown experimentally in studies of oscillating cylinders [6], [7], [8], [9]. Vortex-induced vibrations are thus a response problem as opposed to flutter being a stability problem.
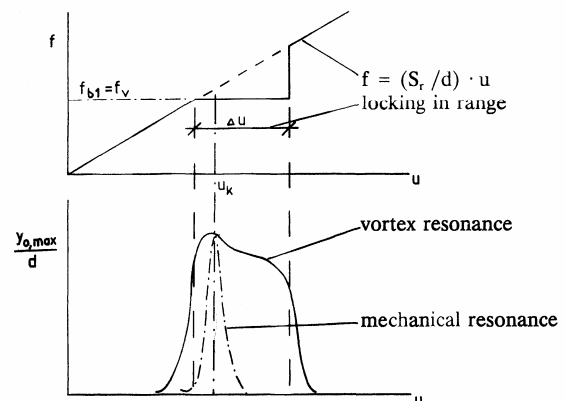

Figure 2. Locking-In Effect and Comparison Between Vortex and Mechanical Resonance, [4]
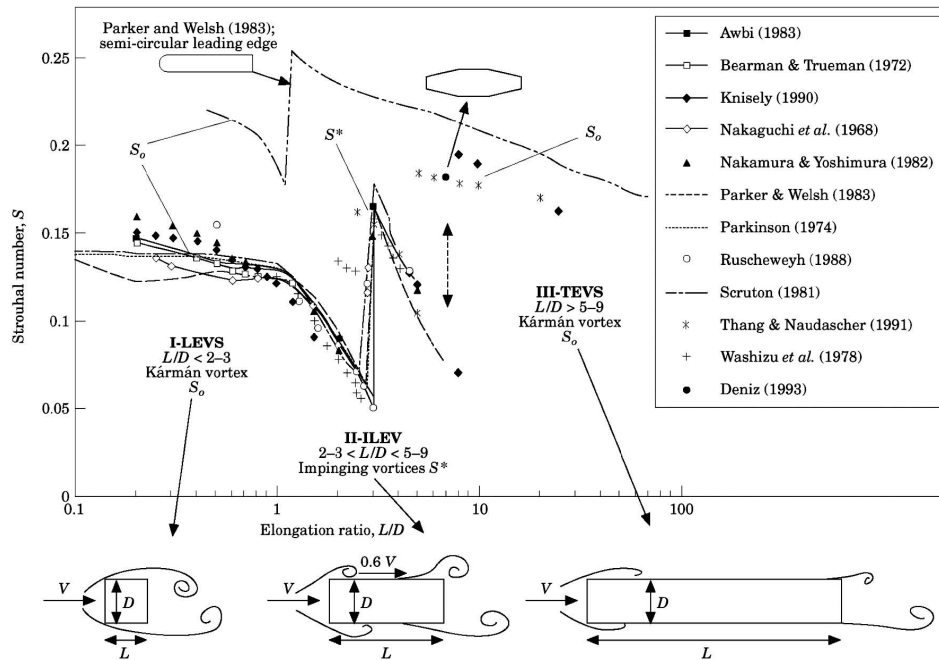
Figure 3. Classes of Vortex Formation Observed with Increasing Elongation of Different Prismatic Bodies,[3,11]: Class I Leading-Edge Vortex Shedding; Class II Impinging Leading Edge Vortices; Class III Trailing-Edge Vortex Shedding.

Vortex resonance occurs only within a limited range of wind speed. The band width of that range depends on the characteristic of the vortex resonance curve, which is influenced by the Reynolds number for circular cylinders. It is clear from the physical understanding of the separation process that viscosity and free stream velocity have an important influence and the can be described by the Reynolds number

$$\mathrm{Re} = \frac{u.d}{\nu}, \qquad [1]$$

wherin u - undisturbed mean flow velocity of the wind; d - characteristic length, diameter or cross-wise dimension of the bluff body; $\nu = \dfrac{\mu}{\rho}$ - kinematic viscosity, depending on the temperature and pressure.

The Reynolds number thus expresses the ratio between the inertia force and the friction force acting on the fluid. If, for example, the flow past a circular cylinder is studied, a great variety of changes in the nature of the flow occur with an increasing Reynolds number.

Generally, the process of vortex shedding and its dependence on the Reynolds number is highly complex which makes analytical as well as numerical treatment very challenging as will be shown in more detail later. A comprehensive overview of the vortex shedding phenomenon and its different modes has been presented by Zdravkovich [10].

Since vortex shedding exerts a fluctuating force on the body, which is of particular interest when the body can be excited to oscillations, Strouhal [1] defined a dimensionless shedding frequency, the Strouhal number, to characterize this process:

$$S_r = \frac{d.f_v}{u}, \qquad [2]$$

where d - diameter or cross-wise dimension of the body; f_v - vortex shedding frequency.

According to Strouhal's observations, subsequent investigations found the Strouhal number to be highly dependent upon the cross-sectional geometry of the body and accordingly focused on determining so called universal Strouhal numbers, which would be independent of the geometry. Figure 3 shows a compilation by Deniz and Staubli [11], which compares results obtained in investigations on the effect of body geometry on the vortex shedding process. The sudden jumps in the Strouhal number occurring at elongation ratios of approximately L/D=2–3 and L/D=4-7 mark the limits of the three flow regimes as illustrated due to the reattachment of the separated flow. The phenomenon vortex shedding was especially investigated for cylinders with a circular cross section, though other cross-sectional shapes will shed regular vortices, too. The vortex shedding on a circular cylinder is highly Reynolds number dependent. With an increasing Reynolds number in the transcritical range, the flow separation becomes more and more regular once again and the vortex street is reestablished. The exciting force increases respectively and this is the reason for dangerous vortex-excited vibrations.
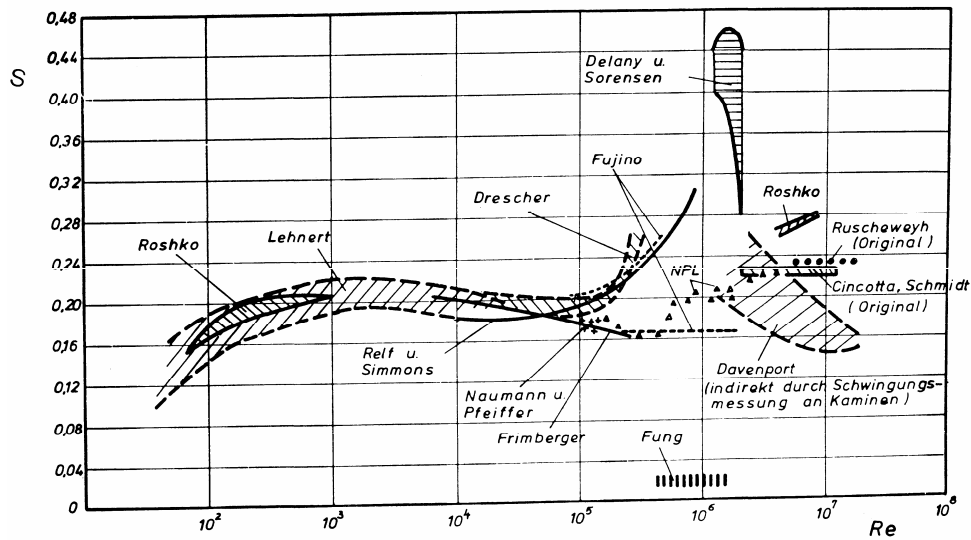
Figure 4. Strouhal Number for Circular Cylinders versus Reynolds Number, [12]

The Strouhal number for a circular cylinder is also strongly dependent on the Reynolds number (Figure 4).

In a recent investigation of the vortex shedding process, Nakamura [13] carried out experiments to compare the different universal Strouhal numbers. He stressed the importance of an afterbody, the presence of which significantly alters the structure of the vortex formation region and seems to render Roshko's ([14], [15]) universal Strouhal number inapplicable.

3. THE AIM OF THE INVESTIGATION

The aim of this investigation is to propose a methodology for studying the vortex excited vibrations in an aerial ropeway with gondolas with stiff connection between the cabin and the hanger. The first step is to predict the frequency of the vortex aerodynamic forces and then to calculate the resulting oscillations of the cabins. It is only the beginning of research aiming to create a methodology for designing aerial ropeways whose characteristics enable avoiding such excitation. This is a serviceable problem, because the levels of vibrations need to be limited, not only to avoid dangerous levels, but as well as to ensure the safety and comfort of the passengers and to avoid fatigue problems in the long term.

4. DYNAMIC MODEL OF THE STRUCTURE

4.1. Dynamic model of the ropeway span

The first step in establishing a dynamic model of a bicable ropeway is to analyze the working principle of the system ([16]). A bicable ropeway works with a certain number of cabins fixed to the haul cable by operationally releasable clamping devices, which can grip the haul cable at any point and therefore enable the setting of various sequential intervals between the

individual gondolas. The speed of the gondolas through the stations decreases and thus enables easy entrance and exit of the passengers. Before exiting the station, the gondola is accelerated to the constant haul cable speed. Outside the station area the cables are led over line support structures, the track cable on saddles (track cable saddle), and the haul cable on support rollers. The drive for the haul cable is provided by the electric motor-driven sheave.

It is assumed that the cross oscillation of the cabins and the movement of the cables in one span between two towers is not transmitted to the next span. Thus the numerical studies can be reduced to one span (Figure 5) of the track. In normal operation, the gondolas move along the span with constant velocity. The trajectory along the span follows the elastic line of the track cable, influenced by the horizontal tension force, the dead weight of the cable and the gondolas. It is also assumed that the elastic line of the track cable is constant and fixed in a vertical direction. That means the absence of vertical oscillation effects or swinging of the cabins in the x-z plane.
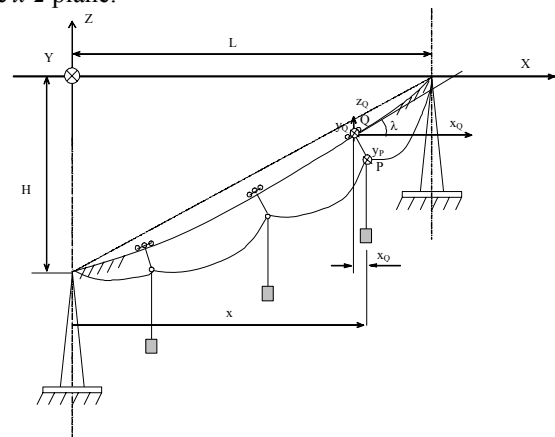

Figure 5. Scheme of a Span of the Bicable Ropeway

4.2. Dynamic model of the gondola, [16]

Every gondola is modeled as a mechanical system with two degrees of freedom—rotation angle φ and horizontal movement of the connection between the track cable and the gondola—y_T (Figure 6). Changes in the inclination angle of the track cable λ (Figure 5), cause changes in the vertical distance between both cables, and consequently in the inertia moment of the gondola towards axis x_Q. The gondola's oscillations in the vertical plane x-z are neglected and as a result it can be assumed that the relative movement of the gondola is in plane y-z. This movement is caused by the vortex, which acts on the cabin W_K, dead weights of the gondolas, including passengers (G_i) and the reactions of the cables. The elastic forces of the cables are modeled by springs with changing stiffness. They are the horizontal force between the track cable and the gondola (acting at point Q) and the force in the clamp (acting at point P).

In accordance with the relation between gondola distance l to the distance between the towers L (Figure 5) a certain number of gondolas are moving in the span. In this mechanical system, all damping forces are very minor, therefore they are neglected. The differential equation for each gondola is as follows

$$\begin{bmatrix} A & B \\ B & C \end{bmatrix} \begin{Bmatrix} \ddot{\varphi}_i \\ \ddot{y}_{Ti} \end{Bmatrix} = \begin{Bmatrix} f_1 \\ f_2 \end{Bmatrix} \qquad [3]$$

where: φ_i – angle of rotation of gondola number i round axis x_Q;

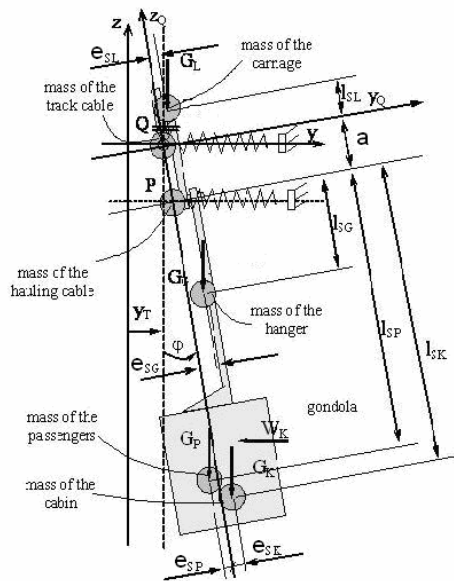 y_{Ti} - horizontal coordinate of the connection between the gondola number i and the track cable (point Q);

A, B, C – coefficients, depending on mass and geometric characteristics of gondola, including passengers inside. Certain parts of the mass of the hauling cable and the mass of the track cable are added to the gondola number i.

The generalized forces f_1 and f_2, including wind vortex W_K and the elastic forces from the cables, are time dependent as well as position dependent functions.

Having in mind the nature of the vortex phenomenon, (Figure 1) the vortical exciter can be modeled like a harmonic force $W_K = F_{\max}.\sin 2\pi.f.t$, where f is the vortex frequency in Hz. This force acts crosswise on the rope span. Its maximum is

$$F_{\max} = c_{lat}.\frac{\rho}{2}.u^2.A_{cab}, \qquad [4]$$

where ρ - air density;

   A_{cab} - cross section area of the cabin;

   c_{lat} - exciting force coefficient. It must be measured by model tests or full scale measurements. For circular cylinders it is a function of Reynolds number. The relation between the basic exciting force coefficient c_{lat} versus the Reynolds number, according to Euro Code 1, part 6 for circular cylinders is given in Figure 11 [12].

5. NUMERICAL SIMULATION

5.1. Numerical data of the studied ropeway span

Later presented in the results of the simulation, the geometric data and specifications of a bicable ropeway, which has been in operation for five years, are used. The results are given for one span of the ropeway track.
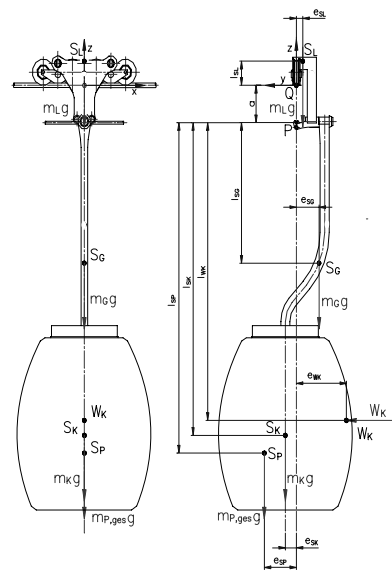

Figure 6. Mechanical Model of a Gondola with Stiff Connected Cabin

Figure 7. Drawing of the Gondola and the People Inside It with All Dimensions

Some of the used parameters of the ropeway are provided in the Table 1.

5.2. Numerical data of the gondolas (Figure 7)

Some of the applied parameters and variables of the geometric characteristics of the gondolas are given in Table 2.

Symbols and values of some other variables used for calculating the vortex excitation can be found in Table 3.

5.3. Calculation of the frequency of the ropeway

At first a harmonic analysis of the ropeway span is performed. The gondolas move along the span with constant velocity. The equation

$$[M]\{\ddot{u}\} + [K]\{u\} = F(t) \qquad [5]$$

for different frequencies of the excitation is solved. The value of the velocity of the gondolas varies between 1 m/s to 6 m/s. The harmonic force is calculated according to the formula

$$F = 10.\sin(2\pi.f.t) \qquad [6]$$

where its maximal value is constant and is equal to 10N and f is the exciting frequency. It varies between 0.1 Hz (period T= 10 s) to 0.6 Hz (T= 1.67 s).

The two degrees of freedom φ_i and y_{Ti} (where i is the number of the gondola) of each gondola are obtained and a third important characteristic, the horizontal coordinate of the mass center of the cabin (Figure 6) $y_{Ki} = y_{Ti} + (a_i + l_{SK})\sin\varphi_i + e_{SK}\cos\varphi_i$, is calculated. The maximal amplitudes of these three parameters are found. It can be seen that the most dangerous velocity is v=2.0 m/s, if velocity v=1.0m/s, which is a very untypical velocity for a ropeway, is excluded (Figure 8). The functions φ_i, y_{Ti} and y_{Ki} versus frequency are shown in Figure 9. It can be seen that the resonance frequency of the ropeway varies round 0.25 Hz (T=4s). As it was measured, the basic natural frequency of a similar gondola is about 0.25 Hz. Vortex oscillations of a gondola in ropeway span with similar characteristics, i.e. $\varphi_i = \varphi_i(t)$, are measured for a velocity of 2.5 m/s ([17],[18], [19]).

Table 1. Parameters of the Ropeway

Symbol	Identification	Values in the cited example	Dimension
Masses and force parameters			
	mass of all passengers in gondola i	80 kg/person	[kg]
	mass of the hauling cable, added to gondola number *i*	calculated for each gondola	[kg]
	mass of the track cable, added to gondola number *i*	calculated for each gondola	[kg]
	dead weight of the hauling cable	61.8	[N/m]
	dead weight of the track cable	126.5	[N/m]
	value of the horizontal projection of the force in the track cable, out of the span	constant	[N]
	value of the horizontal projection of the force in the hauling cable, out of the span	constant	[N]
	elastic force of the reaction of the track cable, due to its horizontal movement, acting over gondola number *i*.	calculated at every integration step	[N]
	elastic force of the reaction of the hauling cable, due to its horizontal movement, acting over gondola number *i*.	calculated at every integration step	[N]
Velocity parameters			
u	velocity of motion of the hauling cable and the gondolas with passengers	varies between 1m/s to 6m/s	[m/s]
Geometric parameters			
L	horizontal distance between the towers (Figure 5)	800	[m]
l	horizontal distance between every two gondolas. (Figure 5)	250	[m]
H	vertical distance between the towers (Figure 5)	300	[m]
λ	the inclination angle of the elastic line of the track cable, due to its dead weight (Figure 5)	time and position dependent variable	[rad]

Table 2. Geometric Characteristics of the Gondolas (Figure 7)

Symbol	Identification	Values in the cited example	Dimension
Masses and force variables			
	mass of the carriage	500	[kg]
	mass of the hanger	150	[kg]
	mass of the cabin	600	[kg]
W_K	horizontal vortical exciter at the cabin $W_K = F_{max} \sin(2\pi.f.t)$		[N]
Geometric variables			
e_{SL}, l_{SL}	coordinates of the mass center of the carriage in coordinate system Qy_Qz_Q (Figure 6 and Figure. 7)		[m, m]
$e_{SG}, l_{SG} + a_i$	coordinates of the mass center of the hanger in coordinate system Qy_Qz_Q (Figure 6 and Figure 7)		[m, m]
$e_{SK}, l_{SK} + a_i$	coordinates of the mass center of the cabin in coordinate system Qy_Qz_Q (Figure 6 and Figure 7)		[m, m]
$e_{SPi}, l_{SPi} + a_i$	coordinates of the mass center of the passengers in coordinate system Qy_Qz_Q (Figure 6 and Figure 7)		[m, m]
$e_{WK}, l_{WK} + a_i$	coordinates of the acting point of the vortical exciter over the cabin W_K in coordinate system Qy_Qz_Q (Figure 6 and Figure 7)		[m, m]
a_i	vertical coordinate of the clamp (point P) of gondola number i, in coordinate system Qy_Qz_Q (Figure 6 and Figure 7)		[m]
i_L	mass inertia radius of the carriage		[m]
i_G	mass inertia radius of the hanger		[m]
i_K	mass inertia radius of the cabin		[m]
i_{Pi}	mass inertia radius of all passengers in gondola i.		[m]

Table 3. Other Variables Used for Calculating the Vortex Excitation

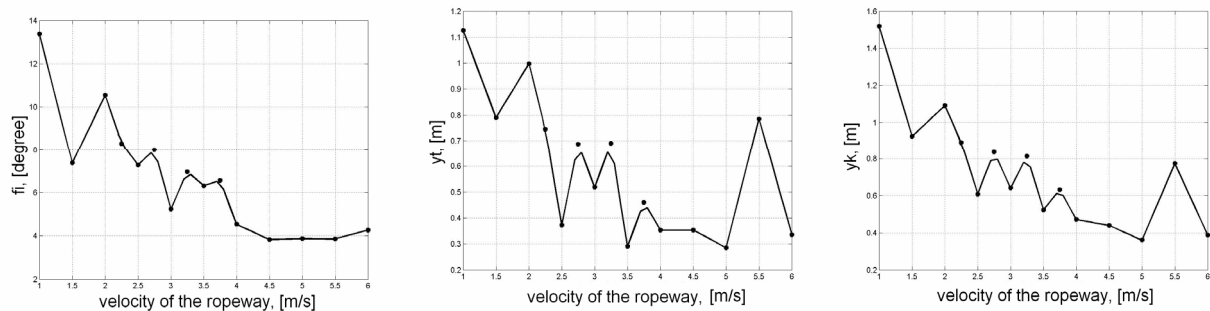| Symbol	Identification	Values in the cited example	Dimension
d	cross-wise dimension of the cabin	2.30	[m]
A_{cab}	cross area of the cabin, exposed to wind exciting	5.83	[m^2]
ν	kinematic viscosity of the air	15.10^{-6}	[m^2/s]
ρ	density of the air	1.25	[kg/m^3]
c_{lat}	exciting force coefficient	dependable	[-]
f	frequency of the vortex	0.1÷0.6	[Hz]
S_r	Strouhal number	0.2	

Figure 8. Maxima of the Studied Parameters φ_i, y_{Ti} and y_{Ki} versus Velocity of the Ropeway

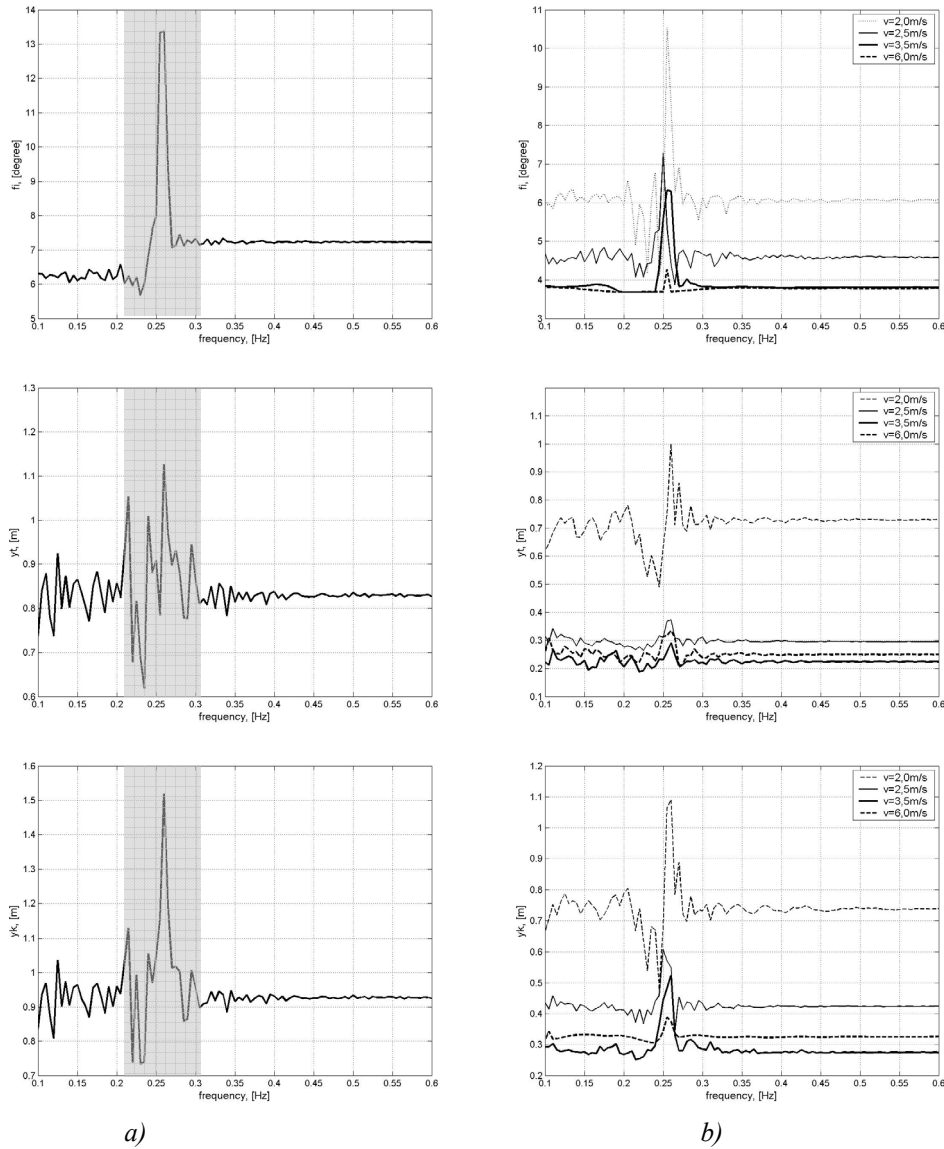*a)*   *b)*

Figure 9. Maxima of the Studied Parameters φ_i, y_{Ti} and y_{Ki}

      a) Versus Frequency for Velocity Varying between $1\,\text{m/s} \div 6\,\text{m/s}$

      b) Versus Frequency for Some Velocities of the Ropeway

5.4. Calculation of Reynolds number

The Reynolds number is calculated according to formula (1). The undisturbed mean flow velocity of the wind u case is accepted to be equal to the speed of the ropeway and varies between 1m/s and 6m/s. The increasing step is 0.25 m/s.

Thus the Reynolds number varies between $1{,}53.10^5$ and $9{,}20.10^5$.

5.5. Calculation of the Strohal number. Establishing the dangerous vortex frequency

It is hard to determine the exact value for the Strohal number. As can be seen in Figure 4, the Strohal number for circular cylinders varies strongly versus Reynolds numbers. For practical engineering purposes for circular cylinders, it is accepted that the Strouhal number is constant and $S_r = 0.2$.

The cabin in our simulation is almost a circular cylinder and according to graphical relation (Figure 4) the Strohal number is between 0.16 and 0.24. So we can calculate the frequency interval of vortex excitation as follows:

$$f_v = \frac{S_r}{d} u \,. \qquad [7]$$

The obtained results are shown in Figure 10. The dangerous zone for the studied ropeway is between the two lines—the lower limit and the upper one. Depending on the velocity of the ropeway, the vortex-excited vibrations can occur if the natural frequency of the structure is inside the limited interval. For our ropeway, it varies between 0.18 Hz to 0.32 Hz (Figure 9a). The zone with high values of the studied parameters is quite broad due to the observed lock-in effect. It is obvious that the velocities for which Vortex excitation can occur are in the interval $2\,\text{m/s} \div 3.5\,\text{m/s}$. Maximal amplitudes of two DoFs and of the horizontal coordinate of the mass center of the cabin for velocities and frequencies inside the vortex area (Figure 10) are shown in Figure 12. Usually the velocity of the ropeway is 6 m/s and the vortex frequency is between 0.4 Hz and 0.6 Hz. These values are high above the natural frequency and thus vortex effect for that velocity can not occur in the studied ropeway during its regular operation. So our investigations are more detailed and punctual in the previous zone—a velocity between $2\,\text{m/s} \div 3.5\,\text{m/s}$ (Figure 9b).
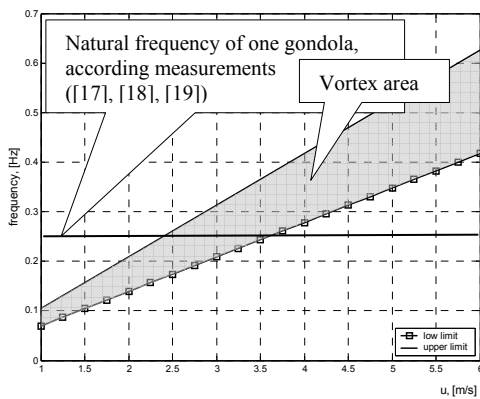

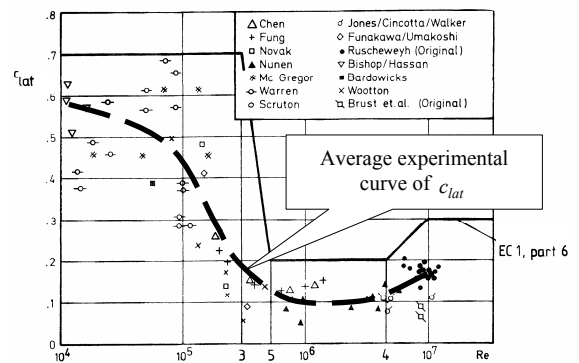Figure 10. Zone of Vortex Frequency versus Velocity of the Movement

Figure 11. Coefficient c_{lat} versus Reynolds Number for Circular Cylinders, [12]
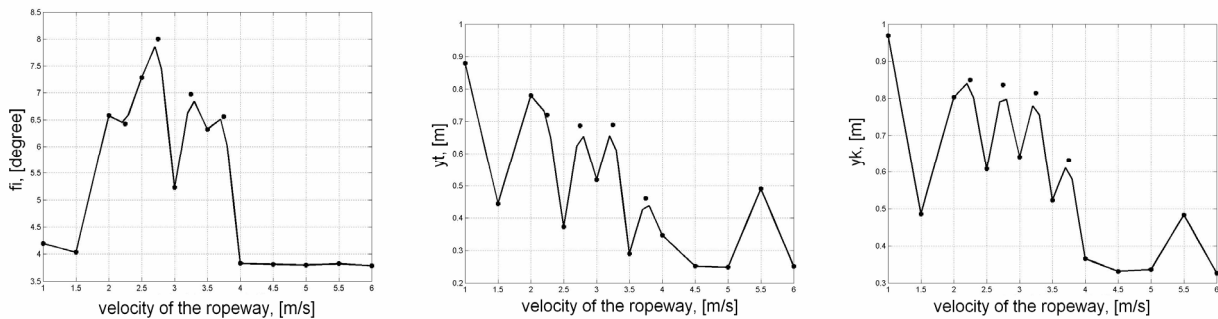

Figure 12. Maxima of the Studied Parameters φ_i, y_{Ti} and y_{Ki} versus Velocity of the Ropeway, Varying in the Dangerous Vortex Area

5.6. Calculation of the amplitude of the vortex exciting force

The maximal vortex exciting force F_{max} is calculated according to (4), where the values of ρ and A_{cab} are given in Table 3. At first, the value of coefficient c_{lat} is taken from the graph in EC1, part 6 and after that similar calculations are done for values taken from the average experimental curve shown in Figure 11 and Figure 13. In Figure 14, the maxima for vortex excitation of the studied parameters (φ_i and $y_{t,i}$) versus velocity and for different curves of c_{lat} are shown.

5.7. Vortex excitation in the studied ropeway span depending on initial conditions

Later on, some graphs of the studied parameters for a ropeway with passengers are presented. The vortical exciter is $W_K = F_{max} . \sin 2\pi . f . t$, where $F_{max} = 25.8750\,\text{N}$ and $f = 0.45\,\text{Hz}$ for graphs in Figure 15a.

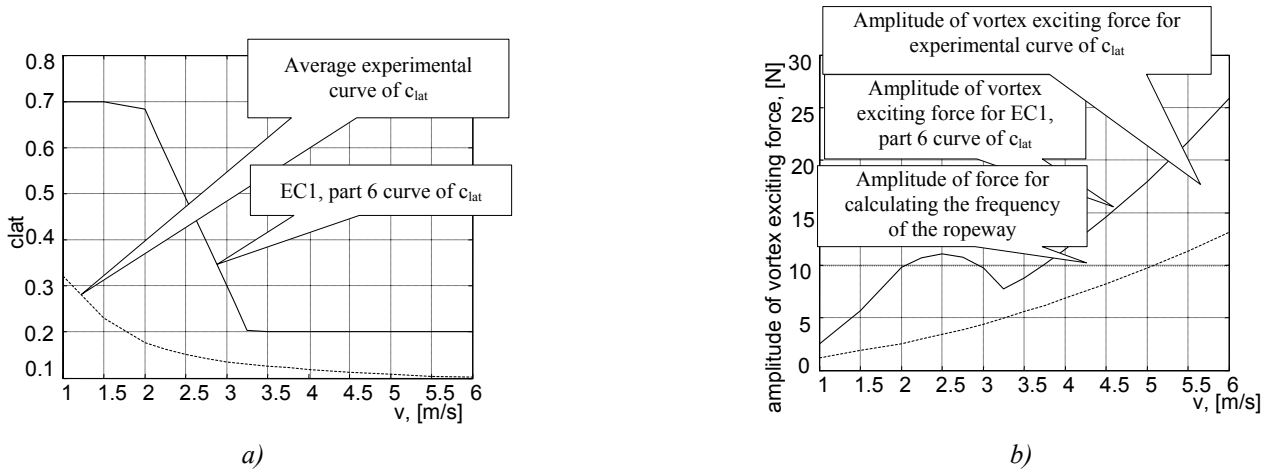*a)*   *b)*

Figure 13. Coefficient c_{lat} and Amplitudes of the Vortex Exciting Force

         a) Coefficient c_{lat} versus Velocity of the Ropeway

         b) Amplitudes of the Vortex Exciting Force versus Velocity of the Ropeway
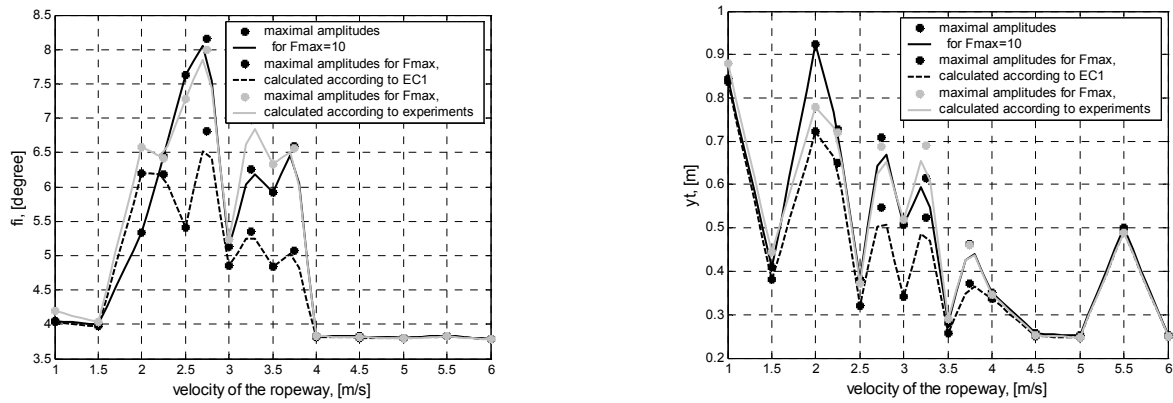

Figure 14. Maxima of the Parameters φ_i and $y_{t,i}$ of the Ropeway for Vortex Excitation versus Velocity of the Ropeway

Table 4. Non-zero Initial Values of the Second Cited Simulation

gondola №	Parameters for thicker gray line			Parameters for narrow black line		
	Initial values of DoFs	sitting passengers	standing passengers	Initial values of DoFs	sitting passengers	standing passengers
gondola № 1	$\varphi_1 = 1°$; $y_{t1} = 0.02\,\mathrm{m}$	5	10	$\varphi_1 = 0°$; $y_{t1} = 0.00\,\mathrm{m}$	5	10
gondola № 2	$\varphi_2 = 2°$; $y_{t2} = -0.03\,\mathrm{m}$	8	7	$\varphi_2 = 0°$; $y_{t2} = 0.00\,\mathrm{m}$	8	7
gondola № 3	$\varphi_3 = -3°$; $y_{t3} = 0.025\,\mathrm{m}$	0	10	$\varphi_3 = 0°$; $y_{t3} = 0.00\,\mathrm{m}$	0	10
gondola № 4	$\varphi_4 = 0.5°$; $y_{t4} = 0.005\,\mathrm{m}$	5	3	$\varphi_4 = 0°$; $y_{t4} = 0.00\,\mathrm{m}$	5	3
gondola № 5	$\varphi_5 = -1°$; $y_{t5} = 0.02\,\mathrm{m}$	1	8	$\varphi_5 = 0°$; $y_{t5} = 0.00\,\mathrm{m}$	1	8
gondola № 6	$\varphi_6 = 1°$; $y_{t6} = 0.005\,\mathrm{m}$	0	1	$\varphi_6 = 0°$; $y_{t6} = 0.00\,\mathrm{m}$	0	1
gondola № 7	$\varphi_7 = 2°$; $y_{t7} = 0.01\,\mathrm{m}$	2	9	$\varphi_7 = 0°$; $y_{t7} = 0.00\,\mathrm{m}$	2	9

$F_{max} = 11.0440\,\text{N}$ and $f = 0.25\,\text{Hz}$ for graphs in Figure 15b. The frequency f is chosen to be inside the interval of vortex frequency (Figure 10) and the amplitude of the vortex force is calculated for coefficient c_{lat}, taken according to EC1. It is observed that for a ropeway with passengers, the influence of this coefficient is not so strong.

The results, obtained by numerical simulations for c_{lat} calculated in accordance with EC1, and the measured values differ by no more than 10 %. The EC1 values are safer. In accordance with the legend in Figure 15, the initial conditions are set to zero (the thicker gray line) or have non-zero initial values (narrow black line) – Table 4.
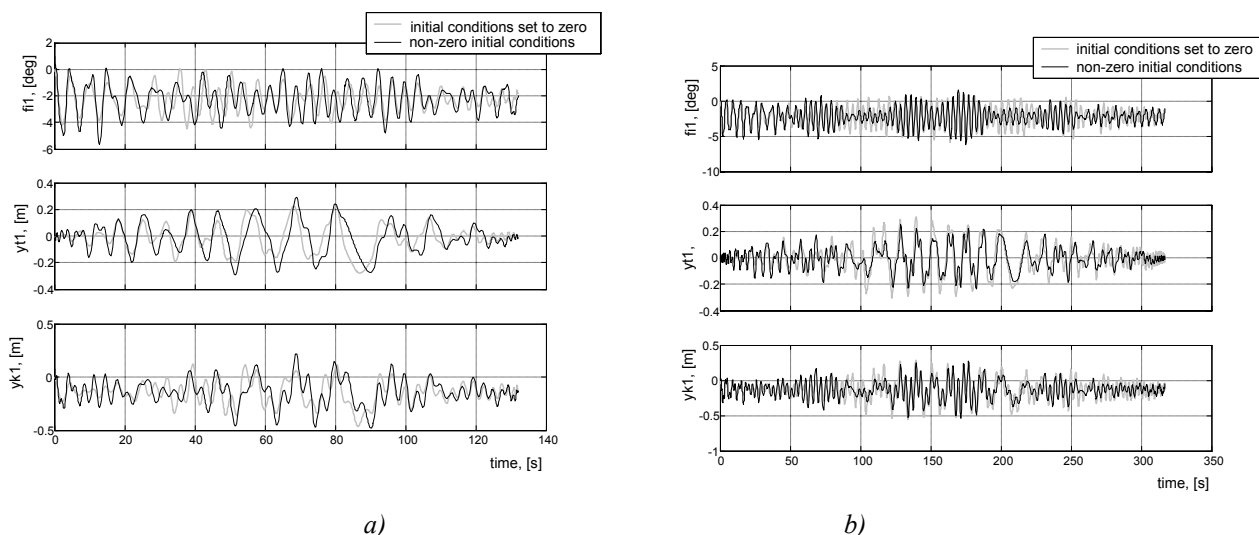

a)   *b)*

Figure 15. Studied Parameters of the Gondola № 1 for Different Conditions versus Time
        a) Velocity of the Ropeway – 6 m/s
        b) Velocity of the Ropeway – 2.5 m/s

6. CONLUSIONS

The created methodology is suitable for studying the vortex excitation in aerial ropeways.
It can be applied for exploring the vortex excitations in various elastic multibody systems. The suggested algorithm:
   • Calculation of the basic natural frequency of the elastic system;
   • Calculation of Reynolds number for the body cross section;
   • Calculation of Strohal number and establishment of the dangerous vortex frequency;
   • Calculation of the amplitude of the vortex exciting force;
   • Influence of initial conditions on the vortex excitation in the studied elastic system;
marks the main stages of such a global investigation.

The dynamic model of an aerial ropeway for studying its vortex dependence is created. It simulates the dynamic reactions of all bodies (the ropes and the gondolas) and visualizes their motion. The comparison between the final numerical results and the experimental data ([17], [18], [19]) shows good consistency. The numerical results are also compared to numerical models created before [16] and the tolerance is again satisfying.
The created models are user-friendly and flexible, i.e. they allow easy changing of the system parameters. Thus they provoke their usage for scientific purposes as well as for engineering calculations.
Thus, this investigation becomes a part of the efforts of scientists to reduce vortex excitation in aerial ropeways [20], and therefore to make them safer and more comfortable.

7. LIST OF SYMBOLS

Reynolds number	$Re,$	-
undisturbed mean flow velocity of the wind	u ,	m/s
kinematic viscosity	v ,	m^2/s
Strouhal number	S_r ,	-
angle of rotation of gondola number i round axis x_Q	φ_i ,	rad
horizontal coordinate of point Q	y_{Ti} ,	m
vortex frequency	f ,	Hz
air density	ρ ,	kg/m^3
cross section area of the cabin	A_{cab} ,	m^2
exciting force coefficient	c_{lat} ,	-

REFERENCES

[1] Strouhal, V. C., *On a particular way of tone generation (German)*, Annalen der Physik und Chemie, Vol. 5, 1878, pp. 216-251

[2] Karman, T., *Ueber den Mechanismus des Widerstandes, den ein bewegter Koerper in einer Fluessigkeit erfaehrt*. Nachr. d. Koeniglichen Gesellschaft d. Wissenschaften, Goettingen (1911), pp. 509-517, (1912), pp. 547-556

[3] Morgenthal G., *Fluid-Structure Interaction in Bluff-Body Aerodynamics and Long-Span Bridge Design: Phenomena and Methods* , Technical Report No. CUED/D-Struct/TR.187, University of Cambridge Department of Engineering

[4] Sockel H., *Wind-Excited Vibrations of Structures*, CISM Courses and lectures N335, International centre for mechanical sciences, Springer Verlag Wien-New York, 1994.

[5] Fung, Y.C., *An introduction to the theory of aeroelasticity*, Dover, 1993.

[6] Feng, C.C., *The measurement of vortex-induced effects in flow past stationary and oscillating circular and d-section cylinders*, M.A.Sc. thesis, University of British Columbia, Vancouver, B.C., Canada, 1968

[7] Griffin, O.M., G.H. Koopmann, *The vortex-excited lift and reaction forces on resonantly vibrating cylinders*, Journal of Sound and Vibration, Vol. 54 (1977), pp. 435-448.

[8] Griffin, O.M., *Vortex-excited cross-flow vibrations of a single cylindrical tube*, ASME Journal of Pressure Vessel Technology, Vol. 102 (1980), pp. 158-166

[9] Griffin, O.M., S.E. Ramberg, *Some recent studies of vortex shedding with application to marine tubulars and risers*, ASME Journal of Energy Resources Technology, Vol. 104 (1982), pp. 2-13

[10] M. M. Zdravkovich, *Different modes of vortex shedding: an overview*, Journal of Fluids and Structures, Vol. 10 (1996), pp. 427-437

[11] Deniz, S., T. Staubli, *Oscillating rectangular and octagonal profiles: Interaction of leading- and trailing-edge vortex formation*, Journal of Fluids and Structures, Vol. 11 (1997), pp. 3-31

[12] Sockel, H.,: Aerodynamik der Bauwerke, Springer, 1985.

[13] Nakamura, Y., *Vortex shedding from bluff bodies and a universal Strouhal number*, Journal of Fluids and Structures, Vol. 10 (1996), pp. 159-171.

[14] Roshko, A., *On the drag and shedding frequency of two-dimensional bluff bodies*, National Advisory Committee for Aeronautics, NACA Technical Note 3169, 1954.

[15] Roshko, A., *On the wake and drag of bluff bodies.* Journal of the Aeronautical Sciences, Vol. 22 (1955), pp. 124-132.

[14] Petrova R. Hoffmann K., Liehl R., *Modelling and simulation of bicable ropeways under cross wind influence*, Mathematical and Computer Modelling of Dynamical Systems, Vol. 13, N1, 2007

[17] Hoffmann K., Liehl R., Querschwingungen von ZUB – Fahrzeugen, Internationale Seilbahnrundschau, 8/2004.

[18] Liehl R., K. Hoffmann, Additional Analysis of Cross *Oscillation Effects at Ropeway During calm Wind Conditions*, 21-st Danubia-Adria Symposium on Experimental Methods in Solid Mechanics, 29.09-02.10.2004 Brijuni/Pula, Croatia

[19] Liehl R., *Vortex excited vibrations at ropeway cabins*, 3-rd Youth Symposium on Experimental Solid Mechanics, Poretta Therme, Italy, 2004.

[20] Staubli T., Humm H., *Massnahmen zur Reduktion stroemungsinduzierter Seilbahnschwingungen*, VDI – Tagung Fluid-Struktur Wechselwirkung, Heidelberg 11/12 Juni, 2002.

Klaus Hoffmann
Technical University of Vienna,
Faculty of Mechanical and Industrial Engineering,
Institute for Engineering Design and Logistics Engineering
Getreidemarkt 9/Stg.4/4.Stk, Vienna – 1060, AUSTRIA

Radostina Petrova
Technical University of Sofia,
Faculty of Engineering and Pedagogy
Department of Mechanics, Machinebuilding and Thermoengineering
bul. "Bourgasko Shosse" N59, Sliven – 8800, BULGARIA
rpetrova123@abv.bg